Journal of Materials Chemistry C

Accepted Manuscript

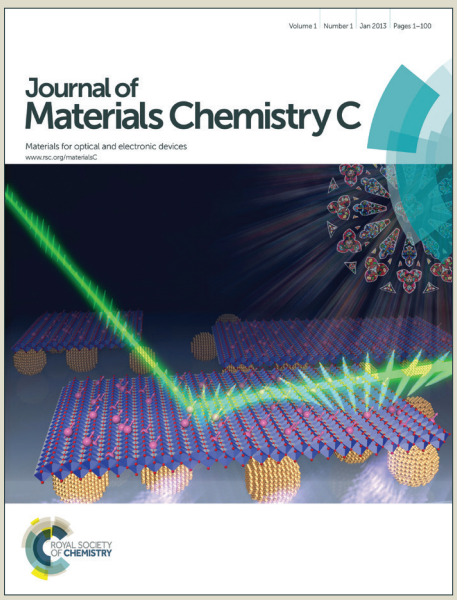

ROYAL SOCIETY OF CHEMISTRY

www.rsc.org/materialsC

High mobility flexible polymer thin-film transistors with octadecyl-phosphonic acid treated electrochemically oxidized alumina gate insulator

Sheng Sun, Linfeng Lan,* Peng Xiao, Zhenhui Chen, Zhenguo Lin, Yuzhi Li, Hua Xu, Miao Xu, Junwu Chen, Junbiao Peng, and Yong Cao

*State Key Laboratory of Luminescent Materials and Devices (South China University of Technology), Wushan Road 381#, Tianhe District, Guangzhou, China. E-mail: lanlinfeng@scut.edu.cn

Flexible solution-processed polymer thin-film transistors (PTFTs) with a low band-gap (LBG) donor−acceptor (D−A) conjugated polymer as the active layer and electrochemically oxidized alumina (AlO_x:Nd) as the gate insulator are fabricated on polyethylene naphthalate (PEN) substrates. The AlO_x:Nd insulator exhibits excellent insulating properties with low leakage current, high dielectric constant and high breakdown field. To improve the interface coupling between polymer active layer and AlO_x:Nd insulator, the AlO_x:Nd insulator is treated with octadecyl-phosphonic acid (ODPA), forming self-assembled monolayers (SAMs) on the surface, and great improvement in TFT performance with the highest mobility of 2.88 $cm^2\ V^{-1}\ s^{-1}$ is attained. The performance improvement is attributed to the smoother surface and lower surface energy of the ODPA-treated AlO_x:Nd compared to those of bare AlO_x:Nd. In addition, the flexible PTFT exhibit only small shifts in the transfer curves at bending curvatures (R) at 30 mm, but the device show larger threshold voltage and higher off current (I_{off}) after bent at R = 5−20 mm, which may be attributed to the damage in the insulator-semiconductor interface.

Introduction

In recent years, considerable interest has been focused on solution-processed polymer thin-film transistors (PTFTs) for their potential applications in flat-panel displays, radio frequency identification tags, e-paper, and sensors due to their low cost, low temperature, large-area manufacture, and flexibility.[1–6] PTFTs with donor−acceptor (D−A) conjugated copolymers have demonstrated high mobility above 10 $cm^2 V^{-1} s^{-1}$.[7–10] Also, some groups achieved mobility above 20 $cm^2 V^{-1} s^{-1}$ after fabricated with macroscopic aligned semiconducting polymers.[11] However, most of these high-mobility PTFTs still need a large operating voltage (50−100 V) and are fabricated on glass or silicon wafers, which limits low-power applications and the intrinsic flexibility of polymer semiconductors. To take advantage of their flexible nature, soluble PTFTs should be fabricated on flexible substrates, e.g., polyimide (PI)[12], polyethylene terephthalate (PET)[13] and polyethylene naphthalate (PEN)[14,15]. However, it is difficult to realize flexible, high-performance PTFTs with low operating voltage, which is highly desirable for low-cost, flexible, organic electronics. One of the most challenging tasks for flexible PTFTs is the preparation of low-temperature and high-reliability gate insulator with good electrical insulation to increase the on/off-current ratio of a TFT and high capacitance to lower the operating voltages and to reduce the power consumption. Poly(4-vinylphenol) (PVP) is one of the most heavily used organic dielectric materials for its good insulating characteristic and excellent film-forming properties with smooth surfaces. However, it should experience high cross-link temperatures at around 200 °C in order to avoid damage during subsequent solution-based processes.[16] Such high temperatures are unacceptable when using low-temperature plastic substrates, like PET or PEN.

Li *et al.*[17,18] have fabricated a high-κ polymer as the gate dielectric of flexible OTFT and got excellent result. Another method to realize low-voltage OTFT operation is to develop several high-κ inorganic or inorganic/organic hybrid blend dielectrics.[19,20] Among high-κ inorganic dielectrics, AlO_x is an outstanding insulator material due to its room-temperature and environmental friendly process, high dielectric constant (8−12), low leakage current, and low cost. For example, Sekitani *et al.*[21,22] and Zschieschang *et al.*[23] have fabricated ultrathin AlO_x using brief oxygen plasma as the gate dielectric. However, the side face coverage characteristics (SFCC) of the dielectric over the side face of the gate electrode (SFGE) is poor and the reliability is not good for the plasma oxidation process.[24−26] In the last few years, we have developed zinc oxide-based TFTs with this anodization technology, attaining high-mobility and high-reliability.[27] In this work, we managed to fabricate flexible PTFTs using AlO_x:Nd as gate insulator on the PEN substrate. However, the surface of AlO_x:Nd film is rough and covered with hydroxyl groups, leading to reduced performance in organic devices fabricated on this unmodified layer. To solve these problems, self-assembled monolayers (SAMs) prepared with octadecyl-phosphonic acid (ODPA) was used to modify the surface of AlO_x:Nd.

Experimental

Metal-insulator-metal (MIM) device fabrication for capacitance characteristics

To evaluate the capacitance at various voltages and frequencies and the leakage current density of AlO_x:Nd with and without ODPA dielectric layers, we fabricated two MIM capacitors with Al:Nd/AlO_x:Nd, modified with or without ODPA/Au, respectively. In this research, test voltages ranged from −18 V to 18 V and frequencies from 1 kHz to 100 kHz.

OTFT device fabrication

Fig. 1a shows the schematic structure of the flexible PTFTs. Firstly, a PEN substrate with a thickness of 50 μm was attached to a glass carrier. Then, SiN_x/photoresist/SiN_x was deposited at 150 ºC as a gas and water barrier on the PEN surface by PECVD and spin-coating alternatively. The thicknesses of the SiN_x and photo-resist were 250 nm and 2000 nm, respectively. A 150-nm-thick Al:Nd (3 wt%) film was deposited with DC sputtering and patterned with conventional photolithography method. Afterwards, Al:Nd film was anodized for 1.5 h to produce a layer of 200-nm-thick AlO_x:Nd on the surface of the Al:Nd film as the gate insulator. After plasma treatment, the substrate was immersed in a 2-propanol solution containing 1 mM ODPA (shown in Fig. 1c) molecules at room temperature (RT) for 8 h. After that, it was removed from the solution, and rinsed thoroughly with 2-propanol, and blown dry with a stream of nitrogen. A low band-gap (LBG) D−A conjugated polymer based on 5,6-difluorobenzothiadiazole (FBT) as the A-unit and quarterthiophene (Th_4) with solubilizing alkyl chains attached on the two terminal thiophene rings as the D-unit (shown in Fig. 1b) was employed as the active material.[28] It was found that FBT-Th_4(1,4) could show unexpected strong interchain aggregation in solutions at RT, whose absorption spectrum in RT solution was almost comparable to that of a thin solid film. FBT-Th_4(1,4) was dissolved in dichlorobenzene (0.8 mg/mL) and spin-coated (2000 rpm) onto ODPA modified AlO_x:Nd with a thickness of 25 nm. Then a 100-nm-thick Au film was thermally evaporated onto the FBT-Th_4(1,4) film through a shadow mask, defining a channel width/length (*W*/*L*) of 500/70 μm. The PTFT characterizations were measured with a semiconductor parameter analyzer (Agilent 4155C) and a probe station at RT in air atmosphere.

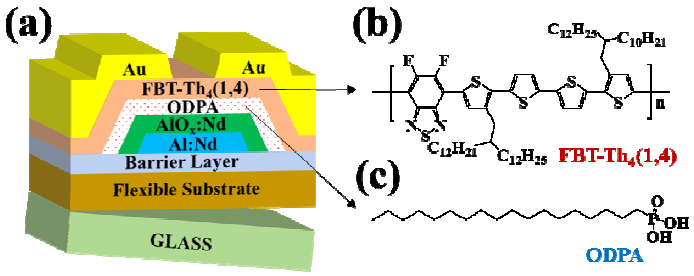

Fig. 1 Schematic diagram of the flexible PTFTs (a); chemical structures of FBT-Th_4(1,4) (b) and ODPA (c).

Results and discussion

To suppress hillock formation and reduce the surface roughness, Al:Nd was used as the gate instead of pure Al.[29] It can be seen from the TEM images that there are Nd clusters (dark areas) segregated in the Al-Nd film. The segregated Nd is important for releasing compressive or tensile strength during bending. The dielectric properties of AlO_x:Nd with and without ODPA were assessed by fabricating MIM capacitors (as shown in Fig.2). The capacitance density (C_i) of the AlO_x:Nd film is 42.0 nF cm^{-2} and the C_i of the AlO_x:Nd with ODPA film is 41.6 nF cm^{-2}.The slow decrease of the measured capacitance with frequency indicating low defect density such as oxygen vacancies in the thin film.[30] Accordingly, the leakage current is relatively low($\approx 2 \times 10^{-8}$ A/cm^2) at an electric field (E) of as high as 3.0 MV/cm, which was lower than those of many other high-κ dielectrics, and ±2 mm under gate field of 2 MV/cm, (not shown) showing good bending flexibility and reliability. These results showed that anodized AlO_x:Nd with ODPA is suitable for use in a gate dielectric layer.

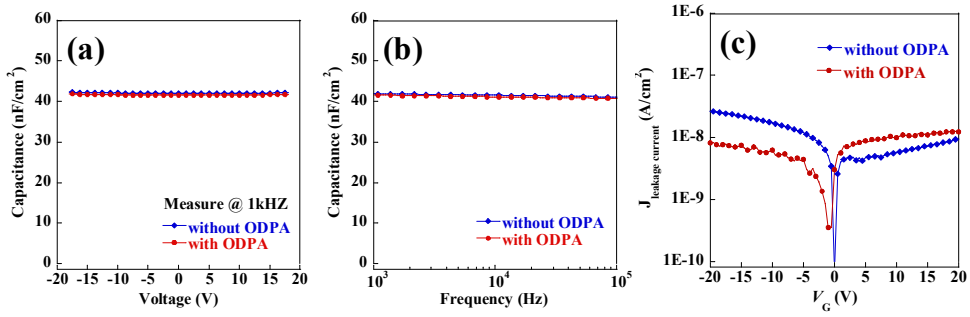

Fig. 2 Capacitance *vs.* voltage plots measured at 1kHz (a) and capacitance *vs.* frequency plots measured at 50 mV (b) for AlO_x:Nd with and without ODPA. (c) Leakage current density *vs.* voltage for AlO_x:Nd with and without ODPA.

Although the anodic AlO_x:Nd has good insulating properties, the hydroxyl groups on the surface and the relatively high surface roughness are the two main drawbacks for PTFT applications. To solve these problems, the surface of the anodic AlO_x:Nd was modified by ODPA SAM. Fig. 3 displays high-resolution transmission electron microscopy (HRTEM) images with the ODPA-treated OFET cross-section to examine the interface of the thin film layers. It can be seen that the insulator-semiconductor interface was uniform and continuous without pinholes or hillocks. The thicknesses of Al:Nd, AlO_x:Nd and FBT-Th_4(1,4) were measured to be 150, 200 and 25 nm, respectively, which were closed to those measured with ellipsometer or step profiler. The fast Fourier transform (FFT) pattern for FBT-Th_4(1,4) is indicated in the inset of Fig. 2c, revealing the presence of nanocrystalline domains.

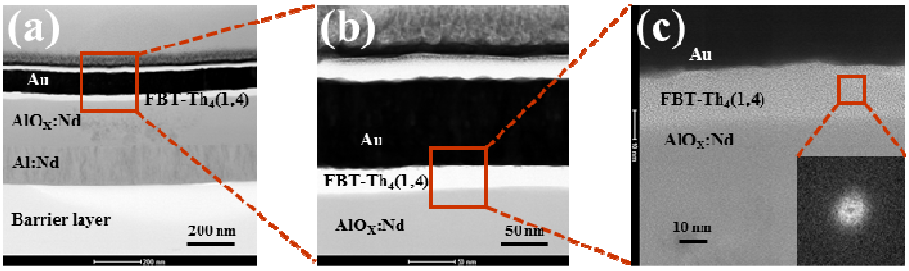

Fig. 3 (a) Cross-section TEM morphology of ODPA-treated OTFTs, (b) magnified image of the boxed region in (a) showing fringes with a 250 nm spacing, (c) HRTEM image of the boxed region in (b) showing fringes with a 80 nm spacing; inset: FFT pattern obtained from the FBT-Th$_4$(1,4) layer.

The ODPA SAM is too thin to be distinguished in the TEM images. Thus, energy dispersive X-ray spectroscopy (EDS) experiments were performed to confirm the existence of the ODPA SAM. Three different points were detected, and signals belong to phosphorus can only be detected in the insulator-semiconductor interface, as shown in Fig. 4. Therefore, it can be deduced that a SAM with ODPA was formed in the surface of AlO_x:Nd.

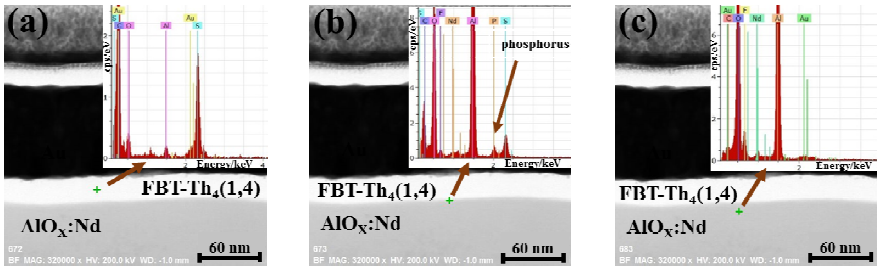

Fig. 4 EDS point scan profiles from (a) the FBT-Th$_4$(1,4) layer, (b) the insulator- semiconductor interface and (c) the AlO_x:Nd layer.

Fig. 5a shows the output characteristics of FBT-Th$_4$(1,4) TFTs on PEN substrates. The device exhibited typical p-channel saturated behaviour with an operation voltage of 18 V, lower than

those of many other PTFTs with traditional low-κ gate insulators. Fig. 5b shows the corresponding transfer characteristics. The threshold voltage was ≈−5.4 V and the on to off current ratio (I_{on}/I_{off}) is ≈10^5. The highest field-effect mobility (μ) of 2.88 $cm^2\ V^{-1}\ s^{-1}$ and the average mobility of ≈1.10 $cm^2\ V^{-1}\ s^{-1}$ were attained when measuring 20 devices (Fig. 5c). It was worth noting that the PTFT device without ODPA treatment showed a mobility of only 0.24 $cm^2\ V^{-1}\ s^{-1}$ (not shown). Moreover, the hysteresis was reduced from 2.5 to 0.3 V after ODPA modification, implying that the hydroxyl groups of AlO_x:Nd are reduced after modified with ODPA.

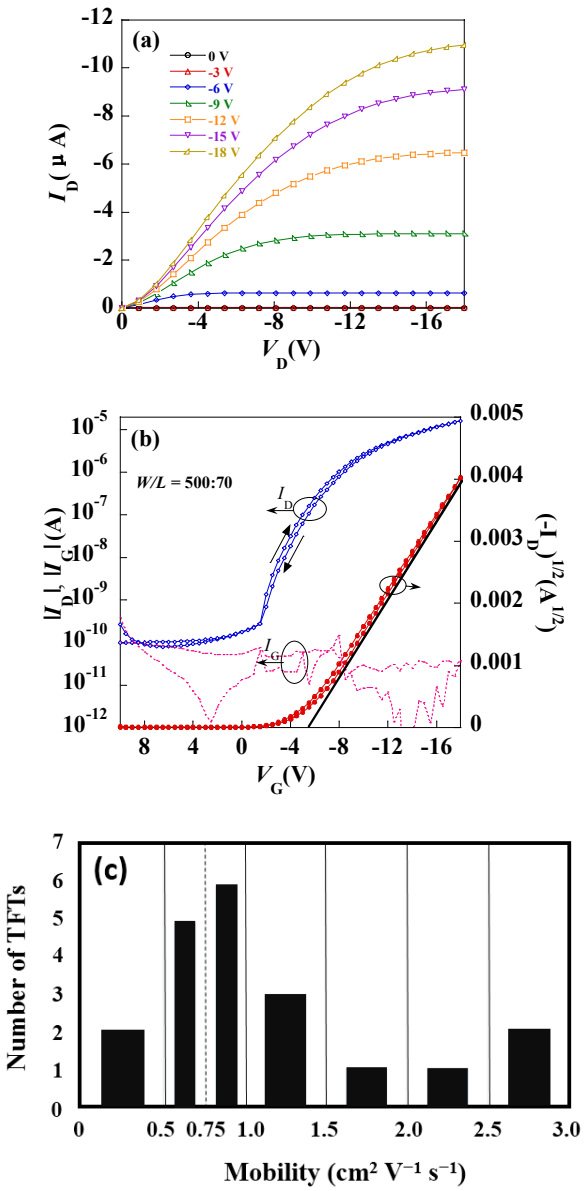

Fig. 5 Output (a) and transfer (b) characteristics of FBT-Th_4(1,4) TFTs with anodic AlO_x:Nd gate insulators modified by ODPA. (c) The mobility distribution of 20 devices.

The performance enhancement by ODPA modification was ascribed to the changes of surface roughness and surface energy of the anodic AlO_x:Nd gate insulators. The surface roughnesses of the AlO_x:Nd before and after ODPA modification were evaluated by atomic force microscope (AFM) experiments. Fig. 6a and b show the AFM images of AlO_x:Nd without and with ODPA

modification layer, respectively. The root mean square (RMS) roughness of AlO_x:Nd was reduced from 3.6 to 2.0 nm after modified with ODPA. The gate insulator with rough surface is believed to reduce mobility in organic semiconductors due to the disorder induced in the accumulation order. Furthermore, the surface roughness of gate insulator has an important effect on the morphology of the organic semiconductors deposited on it, and can disturb π–π stacking, which is critical to efficient charge transport.[31] Fig. 6c and d show the AFM images of FBT-Th_4(1,4) on bare AlO_x:Nd and ODPA-treated AlO_x:Nd, respectively. It was seen that the average grain size of FBT-Th_4(1,4) on ODPA-treated AlO_x:Nd was larger than that of FBT-Th_4(1,4) on AlO_x:Nd. Therefore, the ODPA treatment was good for the grain growing.

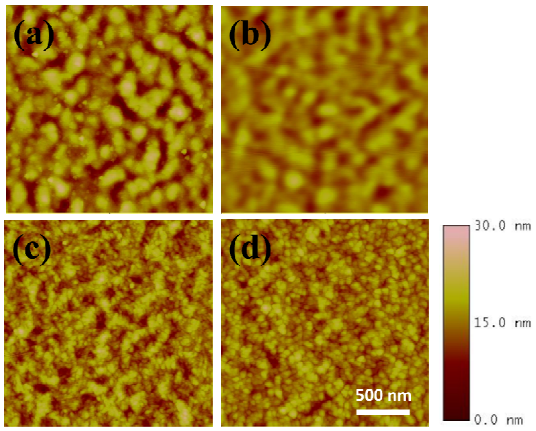

Fig. 6 AFM images of bare AlO_x:Nd (RMS 3.6 nm) (a), ODPA-treated AlO_x:Nd (RMS 2.0 nm) (b), 25-nm-thick FBT-Th_4(1,4) (RMS 3.0 nm) on AlO_x:Nd (c), and 25-nm-thick FBT-Th_4(1,4) (RMS 2.4 nm) on ODPA-treated AlO_x:Nd (d).

It is known that there are lots of hydroxyl groups on the surface of oxide films, indicating that the surface energy of AlO_x:Nd is high. In general, high surface energy is not good for carrier transport in organic TFTs.[32] To evaluate the surface energy of AlO_x:Nd with and without ODPA treatment, water contact measurement was performed. Fig. 7a and b show the water contact angle

measurement images of bare AlO_x:Nd and ODPA-treated AlO_x:Nd, respectively. The water contact angle for bare AlO_x:Nd was 66º, showing hydrophilic characteristic which originated from the hydroxyl groups on the surface. After ODPA treatment, the water contact angle increased to 103º. According to the Young's equation,[33] the surface energy greatly reduced after ODPA modification. Therefore, ODPA treatment can reduce the surface roughness and lower the surface energy, and in turn, improve the performance of PTFTs.

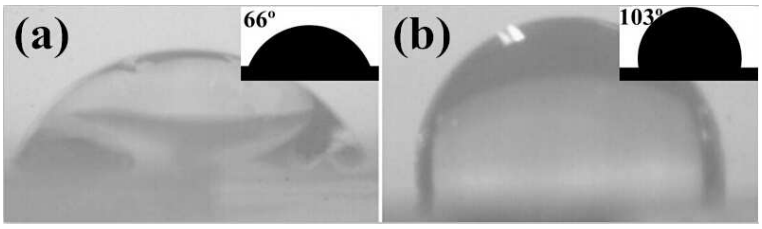

Fig. 7 Water contact angle measurement images of bare AlO_x:Nd (a), and ODPA-treated AlO_x:Nd (b).

The bending flexibility of FBT-Th_4(1,4) TFTs with ODPA-treated AlO_x:Nd gate insulator is shown in Fig. 8. To test the bending flexibility in a more harsh condition, the transfer curves were recorded at a gate voltage as high as −30 V. The PTFT device exhibited only small shifts in the transfer curves at bending curvatures (R) larger than 30 mm, but the device decayed apparently with larger threshold voltage and higher off current (I_{off}) after bent at R = 5−20 mm, which may be attributed to the damage in the insulator/semiconductor interface.

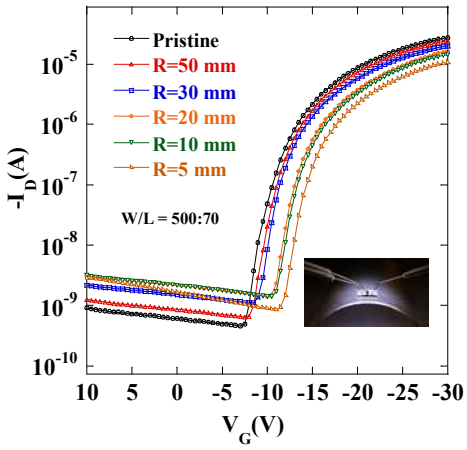

Fig. 8 Transfer characteristics of FBT-Th$_4$(1,4) TFTs with ODPA-treated AlO$_x$:Nd gate insulator under bending conditions. Inset: the image of equipments in bending test.

Conclusions

In summary, flexible PTFTs on a PEN substrate with ODPA-treated electrochemically oxidized AlO$_x$:Nd gate insulator and FBT-Th$_4$(1,4) active layer were fabricated. The AlO$_x$:Nd insulator exhibited excellent insulating properties with low leakage current, high dielectric constant and high breakdown field. OTFTs without ODPA exhibited a mobility of 0.24 cm^2 V^{-1} s^{-1}, while the one with ODPA exhibited higher mobilities with the highest mobility of 2.88 cm^2 V^{-1} s^{-1}. The better performance of the ODPA-modified OTFT was attributed to the smoother surface and lower surface energy of the ODPA-treated AlO$_x$:Nd. The surface roughness of AlO$_x$:Nd reduced from 3.6 to 2.0 nm after modified by ODPA. Meanwhile, the water contact angles were 66º and 103º before and after ODPA treatment, respectively, implying lower surface energy after ODPA modification. In addition, the ODPA-modified OTFT was able to maintain the relatively stable performance under a certain degree of bending. These results indicate that ODPA-treated AlO$_x$:Nd represents a promising approach for the gate insulator for flexible PTFTs.

Acknowledgements

The authors are grateful to the National "863" Project of China (Grant No. 2014AA033002), the National "973" Project of China (Grant No. 2015CB655000), the National Natural Science Foundation of China (Grant Nos. 61204087, 51173049, U0634003, 21225418, and 60937001), the Pearl River S&T Nova Program of Guangzhou (Grant No. 2014J2200053), the Guangdong Province Science and Technology Plan (Grant No. 2013B010403004), the Fundamental Research Funds for the Central Universities (Grant No. 2014ZM0003, and 2014ZZ0028), the Specialized Research Fund for the Doctoral Program of Higher Education (Grant No. 201201721 20008), the National Laboratory for Infrared Physics Open Project (M201406), and the Guangdong Innovative Research Team Program (No. 201101C0105067115).

References

1 C. D. Dimitrakopoulos, P. R. L. Malenfant, *Adv. Mater.,* 2002, **14**, 99.
2 A. C. Arias, J. D. MacKenzie, I. McCulloch, J. Rivnay and A. Salleo, *Chem. Rev.,* 2010, **110**, 3.
3 J. Lee, A. Han, H. Yu, T. J. Shin, C. Yang and J. H. Oh, *J. Am. Chem. Soc.,* 2013, **135**, 9540.
4 C. Liao, C. Mak, M. Zhang, H. L. W. Chan and F. Yan, *Adv. Mater.,* 2015, **27**, 676.
5 B. Kang, W. H. Lee and K. Cho, *ACS Appl. Mater. Interfaces,* 2013, **5**, 2302.
6 H. Yan, Z. Chen, Y. Zheng, C. Newman, J. R. Quinn, F. Dötz, M. Kastler and A. Facchetti, *Nature,* 2009, **457**, 679.
7 H. Chen, Y. Guo, G. Yu, Y. Zhao, J. Zhang, D. Gao, H. Liu and Y. Liu, *Adv. Mater.,* 2012, **24**, 4618.
8 I. Kang, H. Yun, D. S. Chung, S. Kwon and Y. Kim, *J. Am. Chem. Soc.,* 2013, **135**, 14896.
9 W. Li, W. S. C. Roelofs, M. M. Wienk and R. A. J. Janssen, *J. Am. Chem. Soc.,* 2012, **134**, 13787.
10 J. Li, Y. Zhao, H. S. Tan, Y. Guo, C. Di, G. Yu, Y. Liu, M. Lin, S. H. Lim, Y. Zhou, H. Su and B. S. Ong, *Sci. Rep.*, 2012, **2**, 754.
11 H. Tseng, H. Phan, C. Luo, M. Wang, L. A. Perez, S. N. Patel, L. Ying, E. J. Kramer, T. Nguyen, G. C. Bazan and A. J. Heeger, *Adv. Mater.*, 2014, **26**, 2993.
12 L. M. Dumitru, K. Manoli, M. Magliulo, L. Sabbatini, G. Palazzo and L. Torsi, *ACS Appl. Mater. Interfaces,* 2013, **5**, 10819.
13 C. Wang, C. Hsieh and J. Hwang, *Adv. Mater.,* 2011, **23**, 1630−1634.
14 U. Kraft, M. Sejfić, M. J. Kang, K. Takimiya, T. Zaki, F. Letzkus, J. N. Burghartz, E. Weber and H. Klauk, *Adv. Mater.,* 2015, **27**, 207.
15 S. Sun, L. Lan, P. Xiao, Z. Lin, H. Xu, M. Xu and J. Peng, *RSC Advances*, 2015, **5**, 15695-15699.
16 H. Klauk, M. Halik, U. Zschieschang, G. Schmid, W. Radlik and W. Weber, *J. Appl. Phys.,* 2002, **104**, 5259.

17 J. Li, D. Liu, Q. Miao and F. Yan, *J. Mater. Chem.,* 2012, **22**, 15164.
18 J. Li, Z. Sun and F. Yan, *Adv, Mater.*, 2012, **24**, 88.
19 M. Zirkl, A. Haase, A. Fian, H. Schön, C. Sommer, G. Jakopic, G. Leising, B. Stadlober, I. Graz, N. Gaar, R. Schwödiauer, S. Bauer-Gogonea and S. Bauer, *Adv. Mater.,* 2007, **19**, 2241.
20 Y. Ha, S. Jeong, J. Wu, M. Kim, V. P. Dravid, A. Facchetti and T. J. Marks, *J. Am. Chem. Soc.,* 2010, **132**, 17426.
21 T. Sekitani, T. Yokota, U. Zschieschang, H. Klauk, S. Bauer, K. Takeuchi, M. Takamiya, T. Sakurai and T. Someya, *Science*, 2009, **326**, 1516.
22 T. Sekitani, U. Zschieschang, H. Klauk and T. Someya, *Nat. Mater.*, 2010, **9**, 1015.
23 U. Zschieschang, F. Ante, M. Schlörholz, M. Schmidt, K. Kern and H. Klauk, *Adv. Mater.*, 2010, **22**, 4489.
24 L. A. Majewski, M. Grell, S. D. Ogier and J. Veres, *Org. Electron.,* 2003, **4**, 27.
25 L. Lan and J. Peng, *IEEE Trans. Electron Devices,* 2011, **58**, 1452.
26 M. Kaltenbrunner, T. Sekitani, J. Reeder, T. Yokota, K. Kuribara, T. Tokuhara, M. Drack, R. Schwödiauer, I. Graz, S. Bauer-Gogonea, S. Bauer and T. Someya, *Nature*, 2013, **499**, 458.
27 H. Xu, D. Luo, M. Li, M. Xu, J. Zou, H. Tao, L. Lan, L. Wang, J. Peng and Y. Cao, *J. Mater. Chem. C*, 2014, **2**, 1255.
28 Z. Chen, P. Cai, J. Chen, X. Liu, L. Zhang, L. Lan, J. Peng, Y. Ma and Y. Cao, *Adv. Mater.,* 2014, **26**, 2586.
29 L. Lan, M. Zhao, N. Xiong, P. Xiao, W. Shi, M. Xu and J. Peng, *IEEE Electron Device L.*, 2012, **33**, 827.
30 J. H. Park, K. Kim, Y. B. Yoo, S. Y. Park, K. Lim, K. H. Lee, H. K. Baik and Y. S. Kim, *J. Mater. Chem. C*, 2013, **1**, 7166.
31 H. Sirringhaus, *Adv. Mater.,* 2005, **17**, 2411.
32 S. Y. Yang, K. Shin and C. E. Park, *Adv. Funct. Mater.,* 2005, **15**, 1806.
33 Z. Z. You and J. Y. Dong, *Appl. Surf. Sci.,* 2006, **253**, 2102.